



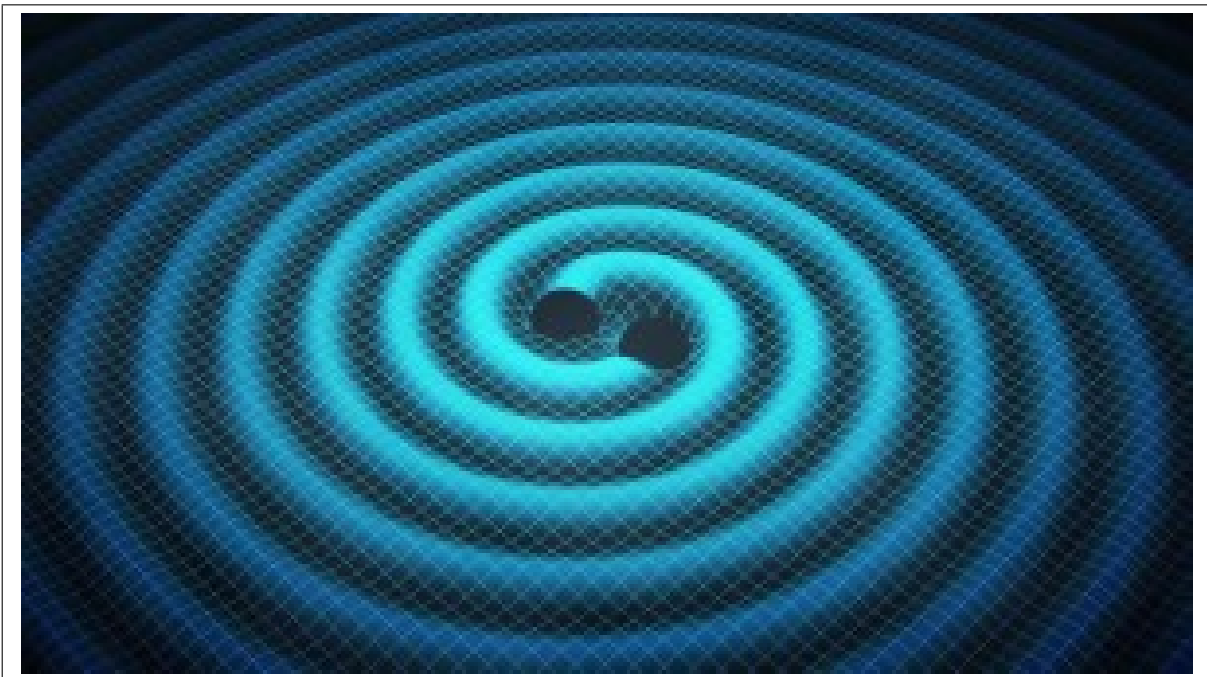
Universiteit Utrecht

Opleiding Natuur- en Sterrenkunde

Gravitational waves from non-circular orbits

BACHELOR THESIS

Rens van Eck



Supervisor:

Prof. Dr. S.J.G. VANDOREN
Institute for Theoretical Physics

June 10, 2020

Abstract

The study of gravitational waves has been a rapidly growing field, and has been dubbed a new era of astronomy. This thesis examines and confirms the frameworks found by previous research to calculate, among others, the strain and power of gravitational waves for circular orbits, and expands this to elliptical orbits and hyperbolic encounters, using general relativity. It is found that the elliptical and circular cases are equivalent up to a factor which depends only on the orbital eccentricity. Furthermore, the case of hyperbolic encounters is examined, and an already detectable hyperbolic encounter is discussed. Lastly, a more accessible derivation Einstein's quadrupole formula is given.

The image on the title page shows an artist's impression of gravitational waves generated by a binary black hole system as the constituent black holes spiral into one another. (Credits: Swinburne Astronomy Productions, found at [2].)

Contents

1	Introduction	1
2	Theoretical background	2
2.1	Linearised gravity	2
2.2	Detection of gravitational waves	4
2.3	Example of gravitational wave source	5
3	Effect of orbital eccentricity	7
3.1	Elliptical orbits ($e < 1$)	7
3.2	Hyperbolic Trajectories ($e > 1$)	13
4	Discussion and conclusions	17
A	Appendix	20
A.1	Gravitational wave strain	20
A.2	Quadrupole formula	21

1 Introduction

More than a century ago, Albert Einstein first predicted the existence of gravitational waves with his theory of general relativity. The study of gravitational waves has since been gaining more and more traction in the last few decades of physics. Where it was first believed that we would never be able to detect these gravitational ripples in spacetime, researchers at LIGO first confirmed in September of 2015 that they had detected the first gravitational waves signal. There has been growing interest in forming theoretical frameworks with which to study these gravitational waves, so as to guide and complement our experimental efforts. In this thesis, we examine a framework to analyse (among others) the power of the gravitational waves emitted by binary black holes (BBH) as they spiral into one another. This has in the past been done for circular orbits and elliptical orbits (see e.g. [18], [4]). We present the circular orbit in section 2.3, as it is a valuable starting point, and then in section 3 present past work on the effect of eccentricity (in bound orbits) on radiated power, fleshing out the derivation a little bit. It used to be thought that any orbital eccentricity a binary might have, would be gone by the time their effects are measurable to us [14]. More recent research shows that dynamically formed binary black hole systems might, however, retain some measurable eccentricity by the time they enter our detector's range [5]. To that end, we calculate an approximation for the timescales regarding the loss of orbital eccentricity, given certain initial conditions. Then, in section 3.2, we present past findings on the calculations of gravitational wave power in hyperbolic encounters of massive objects. We calculate a case which would already be measurable with current technology.

The remainder of this thesis gives some theoretical background in section 2, with special focus regarding linearised gravity and gravitational waves in section 2.1, and how one might go about detecting these exceedingly weak oscillations in spacetime in section 2.2.

2 Theoretical background

Gravitational waves are, in the most basic view, a travelling disturbance in spacetime, which temporarily change its geometry as they pass. Matter that happens to be in a region of spacetime that gravitational waves pass through, will follow this distortion and move in accordance with it. These waves are emitted by massive bodies in acceleration, e.g. by celestial bodies in orbit around one another, which one might compare to the generation of electromagnetic radiation. Electrically charged bodies which are accelerated emit electromagnetic radiation, and in an analogous way, "massively charged" bodies, i.e. bodies with mass, which are accelerated emit gravitational radiation. Both of those types of waves travel at the speed of light in a vacuum.

Einstein first predicted the existence of gravitational waves [9] [10], though he believed they would never be detectable to us, as their effects were believed to be far too weak. However, in 1974, the first indirect evidence for their existence was found, which earned Russell Alan Hulse and Joseph Hooton Taylor, Jr. the 1993 Nobel Prize in Physics [22]. Observations had shown that the change in orbital period of the pulsar in question matched predictions made by general relativity.

As stated before, it's extremely difficult to detect gravitational waves, as their effects are so small. One requires exceedingly sensitive observatories to detect them. In September 2015, the first direct evidence for the existence of gravitational waves was found by LIGO, and the now-famous signal was dubbed GW150914, which was generated by the merger of two black holes [3].

2.1 Linearised gravity

To better understand gravitational waves, we must first gain an understanding of flat spacetime, and how to measure distances in spacetime (see e.g. [13]). The way coordinates are often defined in general relativity, is through use of *four-vectors*. One such four-vector is the position four-vector x^μ , where the Greek upper indices like μ run from 0 to 3, with 0 denoting the time dimension ct , and 1, 2, 3 denoting the Cartesian x, y, z dimensions. Analogously to the Pythagorean theorem in 3 dimensional space, where the distance Δs between two points, or the length s of the vector between them, can be calculated through

$$s^2 = x^2 + y^2 + z^2, \quad (1)$$

we can calculate the length ds of the vector between two so-called *events* in flat spacetime by using

$$ds^2 = -(x^0)^2 + (x^1)^2 + (x^2)^2 + (x^3)^2 = -c^2 dt^2 + dx^2 + dy^2 + dz^2. \quad (2)$$

This is also called the spacetime interval between two events, and is invariant under coordinate transformations (between inertial coordinate systems). We can write this into a shorter form, by utilising the position four-vector x^μ mentioned earlier. Using a matrix η as defined below, we can reconstruct the spacetime interval in flat spacetime:

$$\eta = \begin{pmatrix} -1 & 0 & 0 & 0 \\ 0 & 1 & 0 & 0 \\ 0 & 0 & 1 & 0 \\ 0 & 0 & 0 & 1 \end{pmatrix}. \quad (3)$$

Multiplying from the left-hand side with a four-vector x^μ , and from the right-hand side with another four-vector x^ν , we recover equation (2):

$$\begin{aligned} ds^2 &= \begin{pmatrix} ct & x & y & z \end{pmatrix} \eta \begin{pmatrix} ct \\ x \\ y \\ z \end{pmatrix} \\ &= -c^2 dt^2 + dx^2 + dy^2 + dz^2. \end{aligned} \quad (4)$$

It's become clear that we can use this matrix η to measure distances between events. Objects that we can use to measure distances are called *metrics*, and this particular one is called the Minkowski metric tensor. This can be compacted even further, by introducing the Einstein convention of summation. In this convention, we sum over an index, when it appears as a lower index on one quantity, and as an upper index on an adjacent quantity. As an example, let us take the Minkowski metric from (3), and write down its components:

$$\begin{cases} \eta_{\mu\nu} = 0, & \text{if } \mu \neq \nu \\ \eta_{\mu\nu} = 1, & \text{if } \mu = \nu = 1, 2, 3 \\ \eta_{00} = -1. \end{cases} \quad (5)$$

Now, summing over repeated indices, we can very compactly rephrase equation (2):

$$ds^2 = \sum_{\mu=0}^{\mu=3} \sum_{\nu=0}^{\nu=3} x^\mu \eta_{\mu\nu} x^\nu = x^\mu \eta_{\mu\nu} x^\nu, \quad (6)$$

where we take the summation to be implied due to repeated upper and lower indices, as is usual in the Einstein convention. Now we have all the tools we need to better understand gravitational waves. We start out by constructing new metric, consisting of the flat Minkowski metric, to which we add a small perturbation $h_{\alpha\beta}(x)$:

$$g_{\alpha\beta} = \eta_{\alpha\beta} + h_{\alpha\beta}(x). \quad (7)$$

Let us now consider a simple example of a small perturbation propagating through an otherwise flat spacetime. A simple plane wave propagating in the z-direction is given by the following perturbation:

$$h_{\alpha\beta}(t, z) = \begin{pmatrix} 0 & 0 & 0 & 0 \\ 0 & 1 & 0 & 0 \\ 0 & 0 & -1 & 0 \\ 0 & 0 & 0 & 0 \end{pmatrix} f(t - z). \quad (8)$$

In this equation, $f(t - z)$ is any function of $t - z$ provided $|f(t - z)| \ll 1$. With these perturbations, the geometry of this setup is characterized in a way analogous to equation (4):

$$ds^2 = -c^2 dt^2 + [1 + f(t - z)]dx^2 + [1 - f(t - z)]dy^2 + dz^2, \quad (9)$$

which represents a wave of spacetime curvature propagating in the positive z-direction with speed c , the speed of light. The perturbation in equation (8) is directly related to the detectable "strain" that a gravitational wave causes.

2.2 Detection of gravitational waves

The strain a gravitational wave causes is a measure of how much the wave deforms matter as it propagates through spacetime. As gravitational waves travel away from their source, their energy density decreases, which decreases their strain. The deformation caused by gravitational waves can be expressed for a test mass in the xy-plane as

$$\frac{\delta L}{L} = \frac{1}{2} h_{ij} n^i n^j, \quad (10)$$

where n^i are unit vectors, and we sum over the repeated indices $i, j = 1, 2, 3$. L is the unperturbed length of an object, and δL is the change in length of the object. By the time the gravitational waves from violent encounters such as merging black holes reach Earth, the strain they cause falls to an order of about 10^{-21} or 10^{-22} , which is on the order of a ten-thousandth the width of a proton. The only realistic way of detecting such minute change in length, is by using a device called a laser interferometer, such as in figure 1 below.

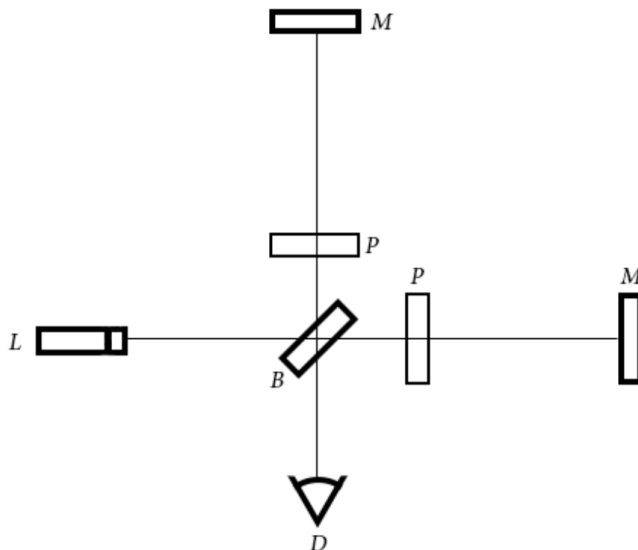


Figure 1: Schematic design of a laser interferometer used to detect gravitational waves. L is a laser source, B a beam splitter, P are partially reflective mirrors, M are mirrors and D is a light detector. (Adapted from [13].)

The components B , P and M are all attached to test masses, which are suspended vertically, to allow them to move in accordance with gravitational waves passing through the detector. When these beams recombine, they will either interfere constructively or destructively, depending on if the lengths of the two arms they travel through, which is the distance between P and M , differ by an odd multiple of a half-wavelength. When gravitational waves pass through these detectors, the length of each arm changes differently depending on the polarisation of the wave, resulting in changing interference patterns. The trouble lies in ensuring that a difference in path length is truly due to a gravitational wave, and not due to various sources of noise.

2.3 Example of gravitational wave source

One of the most common sources of detectable gravitational waves are binary black holes (BBH), which are orbiting around one another. The waves carry off energy, which gradually decreases the distance between them, driving up their orbital frequency until they eventually collide and merge into one black hole, whose mass is less than the sum of the two original black holes. We are interested in finding out how much energy is carried away by gravitational waves, and we shall first examine a simple case of circular orbits.

Let us examine a two-body system of two masses m_1 and m_2 in circular orbit in the xy -plane, around their common center of mass. To this end, we shall make use of a multipole expansion, and argue that in the case of gravitation, we can neglect the dipole contribution. This is due to conservation of linear momentum in an N -body system. The next relevant contribution is the quadrupole moment. The gravitational quadrupole moment Q_{ij} is defined as in [4] (derivation in appendix):

$$Q_{ij} = \int d^3x \rho(x) \left(x_i x_j - \frac{1}{3} r^2 \delta_{ij} \right), \quad (11)$$

where in this equation,

- $r^2 = x^2 + y^2$,
- δ_{ij} is the Kronecker delta,
- $z = 0$, seeing as we're in the xy -plane,
- ρ is the density of the body.

Integrating the ρ term will give us the mass of the body in question, and the second factor turns into an inertia matrix:

$$Q_{ij} = \sum_{A=1,2} m_A \begin{pmatrix} \frac{2}{3}x_A^2 - \frac{1}{3}y_A^2 & x_A y_A & 0 \\ x_A y_A & \frac{2}{3}y_A^2 - \frac{1}{3}x_A^2 & 0 \\ 0 & 0 & -\frac{1}{3}r_A^2 \end{pmatrix}. \quad (12)$$

The sum over A pertains to the bodies in the system, with indices 1 and 2. Using that the bodies orbit their center of mass with a total separation of $r = r_1 + r_2$ between them, with an orbital frequency of $f = \frac{\omega}{2\pi}$, and the parametrisation

$$x = r \cos(\omega t), \quad (13)$$

$$y = r \sin(\omega t), \quad (14)$$

One can show that the quadrupole moment becomes

$$Q_{ij} = \frac{r^2}{2} \sum_{A=1,2} m_A \begin{pmatrix} \frac{1}{3} + \cos(2\omega t) & \sin(2\omega t) & 0 \\ \sin(2\omega t) & \frac{1}{3} - \cos(2\omega t) & 0 \\ 0 & 0 & -\frac{2}{3} \end{pmatrix}. \quad (15)$$

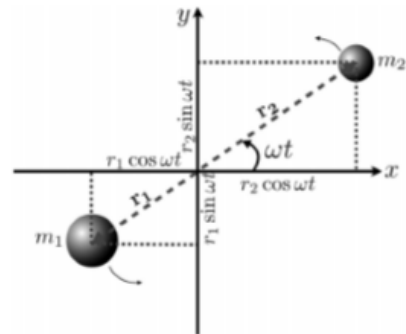


Figure 2: Two-body system of equal masses in circular orbit around their center of mass (from [4]).

We can take out the sum and write the quadrupole moment for the two masses A separately, and insert there a rank-2 tensor I_{ij} in the place of the matrix in equation (15). The total quadrupole moment will still be the sum of the individual moments, which may be written as

$$Q_{ij}^A(t) = \frac{r_A^2 m_A}{2} I_{ij}, \quad (16)$$

where the values of I_{ij} are the values of the matrix above, i.e.,

$$I_{xx} = \frac{1}{3} + \cos(2\omega t),$$

$$I_{yy} = \frac{1}{3} - \cos(2\omega t),$$

$$I_{xy} = I_{yx} = \sin(2\omega t),$$

$$I_{zz} = -\frac{2}{3}.$$

Now performing the sum over $A = 1, 2$, we can compact the equation for the total quadrupole moment (such as (15)), by introducing the reduced mass $\mu = \frac{m_1 m_2}{m_1 + m_2}$, so that the equation reduces to:

$$\begin{aligned} Q_{ij}(t) &= \frac{m_1 r_1^2}{2} I_{ij} + \frac{m_2 r_2^2}{2} I_{ij} \\ &= \frac{1}{2} r^2 \mu I_{ij}. \end{aligned} \quad (17)$$

Now we will try to calculate the power of the gravitational waves, i.e. the energy they are carrying off per unit time. For that, we will use the gravitational wave (GW) strain h_{ij} at a distance d_L from a two-body system like we're concerned with. The GW strain is then given by (derivation in appendix)

$$h_{ij} = \frac{2}{c^4} \frac{G}{d_L} \frac{d^2 Q_{ij}}{dt^2}. \quad (18)$$

The rate at which energy is carried off by gravitational waves is then given by (first found by Einstein [10], and derived accessibly in [1], see appendix.):

$$\frac{dE_{GW}}{dt} = \frac{c^3}{16\pi G} \iint |\dot{h}|^2 dS = \frac{1}{5} \frac{G}{c^5} \sum_{i,j=1}^3 \ddot{Q}_{ij} \ddot{Q}_{ij}, \quad (19)$$

where the integral is to be taken over the surface of a sphere. The third time derivatives that appear in equation (19) can be easily calculated as only the sines and cosines are to be derived w.r.t. time, leaving us with

$$\ddot{Q}_{ij} = 4r^2 \omega^3 \mu \begin{pmatrix} \sin(2\omega t) & -\cos(2\omega t) & 0 \\ -\cos(2\omega t) & \sin(2\omega t) & 0 \\ 0 & 0 & 0 \end{pmatrix}. \quad (20)$$

Now we can evaluate equation (19). We may average the total power radiated by gravitational waves over one period to get rid of the products and sines and cosines this gives us. That'll work out to a total factor of 2, so that, in the end, equation (19) evaluates to

$$\langle P \rangle = \frac{32}{5} \frac{G}{c^5} \mu^2 r^4 \omega^6. \quad (21)$$

3 Effect of orbital eccentricity

3.1 Elliptical orbits ($e < 1$)

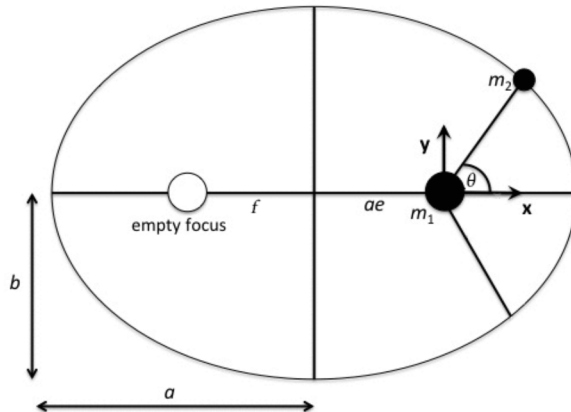


Figure 3: The geometry of an elliptical orbit. Here, a is the semi-major axis, b the semi-minor axis, and f the focal length, i.e. the distance between where a and b meet and a focus. (Adapted from [20].)

The circular case is certainly a valuable starting point, but we know that in reality celestial orbits are often more or less elliptical. To that end, we shall follow roughly the same process as for the circular case, but now specifically incorporate elliptical orbits. We shall treat bound orbits ($e < 1$) and unbound orbits ($e > 1$) separately. Like before, we are interested in knowing the position of the center of mass of the system. The center of mass of a binary system lies in the common focus of the two orbiting bodies, and the bodies are always diametrically opposed with respect to this focus. That is to say, one can draw a straight line between the bodies, and the line will always cross the common focus. Ordinarily, one might be tempted to use the "ordinary" parametrisation of an ellipse, which has its origin on the center of the ellipse, i.e. where its major and minor axes meet. However, we are here interested to know the equation for an ellipse, whose origin lies in one of the foci, shifted by a length f away from the center of the ellipse. To that end, take an ellipse with semi-major axis a lying on the x-axis, semi-minor axis b and focal length $f = \sqrt{a^2 - b^2} = ae$. Then a point (x, y) on the ellipse satisfies

$$\frac{(x + f)^2}{a^2} + \frac{y^2}{b^2} = 1. \quad (22)$$

Multiplying both sides with (ab^2) , substituting the usual $x = r \cos \theta$, $y = r \sin \theta$, and using $1 - \cos^2 \theta = \sin^2 \theta$, we get

$$a^2 r^2 + 2b^2 f r \cos \theta - (a^2 - b^2) r^2 \cos^2 \theta - b^2 (a^2 - f^2). \quad (23)$$

Plugging in the definition of the focal length, we can reduce this to

$$(ar)^2 = (b^2 - fr \cos \theta)^2. \quad (24)$$

Now taking the positive square root gives us the distance of a point (x, y) on the ellipse to a focus:

$$r = \frac{b^2/a}{1 + e \cos \theta} = \frac{l}{1 + e \cos \theta}, \quad (25)$$

with l the semi-latus rectum and e the eccentricity. With this distance, we may easily construct the two orbits of the two black holes. Here we follow largely the approach of Peters & Mathews [18]. Say one black hole has mass m_1 and the other m_2 . The distances of the two bodies to the focus in question is then

$$r_1 = \left(\frac{m_2}{m_1 + m_2} \right) r, \quad (26a)$$

$$r_2 = \left(\frac{m_1}{m_1 + m_2} \right) r. \quad (26b)$$

This we can then use to quickly calculate the components of the quadrupole moment:

$$Q_{xx} = \mu r^2 \cos^2 \theta, \quad (27a)$$

$$Q_{yy} = \mu r^2 \sin^2 \theta, \quad (27b)$$

$$Q_{xy} = Q_{yx} = \mu r^2 \sin \theta \cos \theta. \quad (27c)$$

Like before, $\mu = \frac{m_1 m_2}{m_1 + m_2}$ is the reduced mass. Taking the third time-derivatives and plugging into the equation for the total power radiated, we find

$$P = \frac{8}{15} \frac{G^4}{c^5} \frac{m_1^2 m_2^2 (m_1 + m_2)}{a^5 (1 - e^2)^5} \cdot (1 + e \cos \theta)^4 \cdot [12(1 + e \cos \theta)^2 + e^2 \sin^2 \theta]. \quad (28)$$

Averaging over one orbit once more, we are left with the average power radiated per orbit (in agreement with Peters & Mathews [18] and Turner [23]):

$$\langle P \rangle = \frac{32}{5} \frac{G^4}{c^5} \frac{m_1^2 m_2^2 (m_1 + m_2)}{a^5} f(e), \quad (29)$$

where $f(e)$ is the so-called *enhancement factor*, and is defined by

$$f(e) = \frac{1 + \frac{73}{24}e^2 + \frac{37}{96}e^4}{(1 - e^2)^{7/2}}. \quad (30)$$

Comparing equations (21) and (29), they do not immediately look similar, but implementing the definition of μ and Kepler's third law, they can be shown to be equal up to a factor of $f(e)$ (see equation (38)). That means that the power of gravitational radiation is the same as in the circular case times an enhancement factor that only depends on the eccentricity of the orbit. Figure 4 shows the enhancement factor plotted against e . Take note that $f(e)$ and thereby the power $\langle P \rangle$ rise very steeply as a function of the eccentricity.

As stated before, binary black holes eventually spiral into one another and eventually merge. That means that the semi-major axis of the orbit must decrease over time, and it

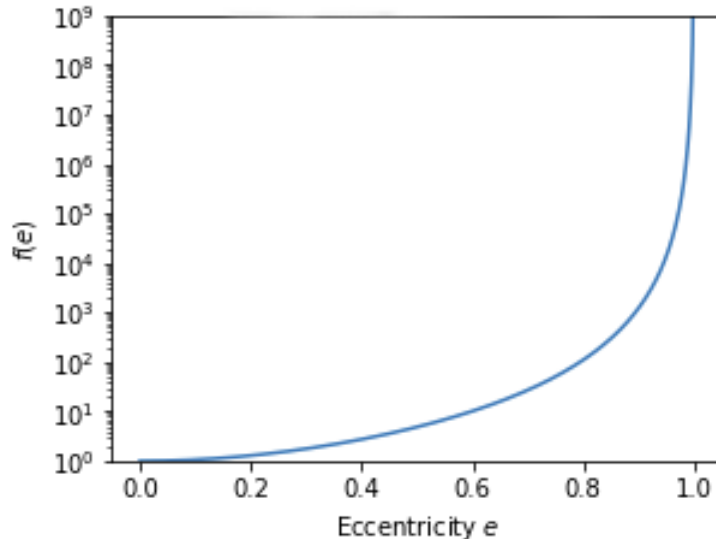


Figure 4: Enhancement factor $f(e)$ as a function of eccentricity [19].

raises the question whether other orbital parameters, such as the eccentricity e , also change with time. In Newtonian theory, we would expect these parameters to be constant in time, but there is evidence that that is not the case. To investigate this theoretically, we follow the approach of Peters (1964) [19]. Sticking with the definition of r as in (25), we will not investigate the perihelion precession. As this investigation has so far been interested in knowing the energies and powers that relate to gravitational radiation, we shall calculate the change in semi-major axis a and eccentricity e from an energy and angular momentum conservation standpoint.

The semi-major axis and the eccentricity are related to the specific orbital energy ϵ and the orbital angular momentum L through the following relations:

$$\epsilon = -\frac{Gm_1m_2}{2a}, \quad (31a)$$

$$L^2 = \frac{Gm_1^2m_2^2}{m_1 + m_2}a(1 - e^2) = \frac{Gm_1^2m_2^2}{m_1 + m_2}l. \quad (31b)$$

We are interested in understanding how these quantities change over time, that is, their time-derivatives. The change of ϵ is precisely energy radiated away by gravitational waves, or equation (29). Similarly, an expression for the time-derivative of the angular momentum can be found:

$$\left\langle \frac{dL}{dt} \right\rangle = -\frac{32 G^{\frac{7}{2}} m_1^2 m_2^2 (m_1 + m_2)^{\frac{1}{2}}}{5 a^{\frac{7}{2}} (1 - e^2)^2} \left(1 + \frac{7}{8} e^2\right). \quad (32)$$

Using equations (29) and (32), we can find expression for the change of a and e in time:

$$\left\langle \frac{da}{dt} \right\rangle = -\frac{64 G^3 m_1 m_2 (m_1 + m_2)}{5 a^3} f(e), \quad (33a)$$

$$\left\langle \frac{de}{dt} \right\rangle = -\frac{304 G^3 m_1 m_2 (m_1 + m_2)}{15 a^4 (1 - e^2)^{\frac{5}{2}}} e \left(1 + \frac{121}{304} e^2\right). \quad (33b)$$

The first things to note are that both of these time-derivatives are strictly negative. For equation (33a), this corresponds to the inspiral phase of a binary black hole system, where the two black holes grow closer and closer together under the influence of gravitational radiation. Equation (33b) is also strictly negative, and shows that the eccentricity of elliptical orbits strictly decreases with time. That means that elliptical orbits circularise over time. It used to be thought that BBH would see their orbit circularise completely by the time they enter the band of Advanced LIGO and Virgo, so that their eccentricity is undetectable [19], [14]. However, more recent research suggests that dynamically formed binary systems that are born at small orbital separations and with large eccentricities, might see their eccentricity remain greater than 0 even into the band of Advanced LIGO and Virgo [5].

We can use eqs. (33a) and (33b) to find a closed expression for the average power radiated per orbit as a function of eccentricity. By dividing the former by the latter, and integrating, we find an expression for the semi-major axis as a function of the eccentricity:

$$a(e) = \frac{c_0 e^{12/19}}{1 - e^2} \left[1 + \frac{121}{304} e^2 \right]^{\frac{870}{2299}}, \quad (34)$$

where the factor c_0 is determined by the initial values of the semi-major axis and eccentricity, a_0 and e_0 respectively [14]:

$$c_0 = \frac{a_0(1 - e_0^2)}{e_0^{12/19} \left[1 + \frac{121}{304} e_0^2 \right]^{870/2299}}. \quad (35)$$

Figure 5 shows a plot of equation (34), with $e_0 = 0.99$. In principle, we could put equation (34) directly into equation (29), but can make future calculations a little easier by taking a step back and rephrasing the relation between eccentricity and the semi-major axis.

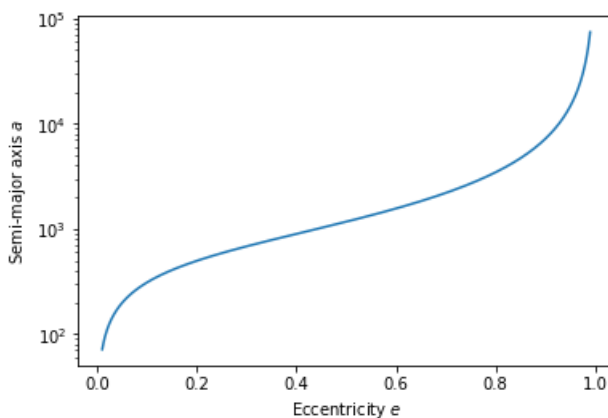


Figure 5: Graph of semi-major axis a versus eccentricity e according to eq. (34) [19].

Explicitly combining equations (34) and (35) can also be used to give rise to a relation between the eccentricity e and the semi-major axis a , and their initial values e_0 and a_0 respectively, as can be found in previous research as well [11]:

$$\frac{a}{a_0} = \frac{1 - e_0^2}{1 - e^2} \left(\frac{e}{e_0} \right)^{12/19} \left[\frac{1 + \frac{121}{304} e^2}{1 + \frac{121}{304} e_0^2} \right]^{\frac{870}{2299}}. \quad (36)$$

This is beneficial, because we can relate the semi-major axis to an orbital frequency ω through Kepler's third law, i.e. $a^3 = \frac{GM}{(2\pi f)^2}$. Then we can calculate how the orbital frequency changes through times, which will then give us a total picture of how the eccentricity of a BBH may change in time.

As stated before, equation (29) can also be modified using Kepler's third law to give an expression that looks like equation (21), times the factor $f(e)$. Applying Kepler's third law to equation (36), where we favour using the angular frequency $\omega = 2\pi f$ and its initial value ω_0 , we find a relation between the angular frequency and the eccentricity:

$$\frac{\omega}{\omega_0} = \left(\frac{1 - e_0^2}{1 - e^2} \left(\frac{e}{e_0} \right)^{12/19} \left[\frac{1 + \frac{121}{304}e^2}{1 + \frac{121}{304}e_0^2} \right]^{\frac{870}{2299}} \right)^{-\frac{3}{2}}. \quad (37)$$

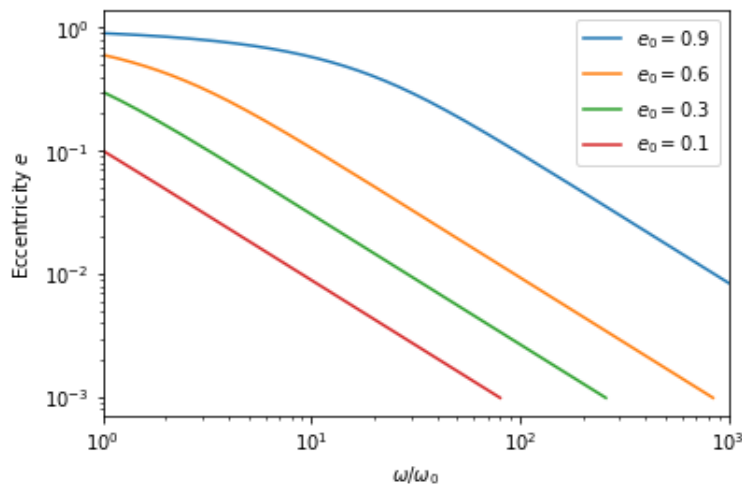


Figure 6: Graph of the evolution of eccentricity versus angular frequency ω/ω_0 , for values of $\omega_0 = 0.9, 0.6, 0.3$ and 0.1 . [11]

Figure 4 above shows the relation between eccentricity and angular frequency as given by equation (37). We can now apply Kepler's third law to equation (29) to find an expression which incorporates ω :

$$\langle P \rangle = \frac{32}{5} \frac{G}{c^5} \mu^2 a^4 \omega^6 f(e). \quad (38)$$

Here, we state that the energy radiated away by gravitational waves decreases the total orbital energy $E_{orb} = -G \frac{M\mu}{2a}$, or put in exact terms:

$$\langle P \rangle = -\frac{dE_{GW}}{dt} = \frac{dE_{orb}}{dt} = \frac{G(m_1 + m - 2)\mu}{2a^2} \dot{a}. \quad (39)$$

With a few extra steps of basic algebra, we find an equation for the time derivative of the orbital frequency:

$$\dot{\omega} = \frac{48}{5} \frac{G^{5/3}}{c^5} \mu (m_1 + m_2)^{2/3} \omega^{11/3} f(e). \quad (40)$$

We can solve this equation for ω , and we find, for $\omega_0 = 2\pi$ rad/s, which is graphed directly below in figure 7 for the same initial values of e_0 as in figure 6:

$$\omega(t) = \frac{1}{\left(1 - \frac{128}{5} \frac{G^{5/3}}{c^5} \mu (m_1 + m_2)^{2/3} f(e) \cdot t\right)^{3/8}}. \quad (41)$$

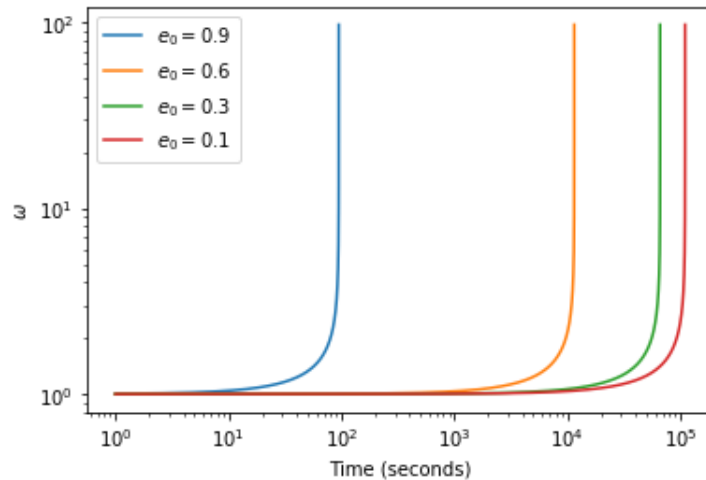


Figure 7: The evolution of the orbital frequency ω with respect to time, for initial values $e_0 = 0.9, 0.6, 0.3$ and 0.1 , and masses $m_1 = m_2 = 30M_\odot$.

We know from measurements on the first detected GW signal, GW150914, that the peak frequency reached by the black holes before merging was about 75Hz, which is half the maximum frequency that the gravitational waves reached [7]. Using figures 6 and 7, we can get estimates for how quickly eccentricity will get lost as the inspiral of the black holes progresses. Taking note that we have set the initial value of the orbital frequency at 1 Hz, we are looking for an increase of roughly 10^2 in the orbital frequency, as that roughly corresponds to a binary black hole system merging. For the case of an initial eccentricity $e_0 = 10^{-1}$, we can see it takes about 10^5 seconds, or roughly 28 hours, for the orbital frequency to go from 1 Hz to an order of 10^2 Hz, which corresponds with the eccentricity going from $e = 10^{-1}$ to roughly $e = 10^{-3}$.

3.2 Hyperbolic Trajectories ($e > 1$)

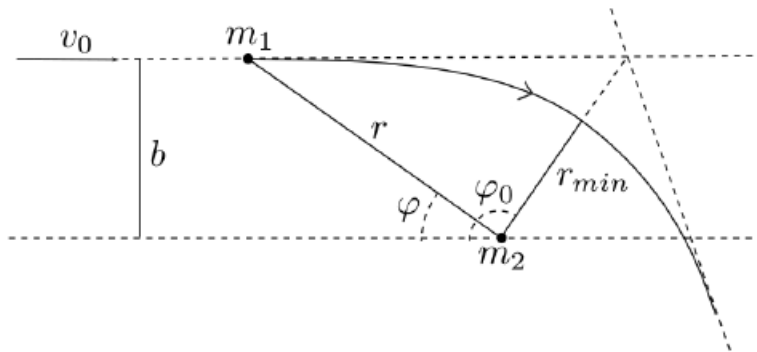


Figure 8: A hyperbolic encounter with some of its defining parameters (from [8]).

To better understand the energy radiated in a hyperbolic encounter of two black holes, we must first define how such a hyperbolic trajectory would look. We largely follow the approach of de Vittori et al [8], with the setup depicted in figure 8. As can be found in textbooks on the matter (such as [15]), the eccentricity e of a hyperbola is related to energy $E = \frac{1}{2}\mu v_0^2$, with v_0 being the velocity of the incoming mass m_1 at infinity and the angular momentum $L = \mu b v_0$, with b the semi-minor axis, of the orbit:

$$e = \sqrt{1 + \frac{2EL^2}{\mu\alpha^2}}. \quad (42)$$

As before μ is the reduced mass, and there is an additional parameter $\alpha = Gm_1m_2$. Similar to the elliptical approach (see equation (25)), the radius of the hyperbolic trajectory is given by

$$r(\phi) = \frac{l}{1 - e \cos(\phi - \phi_0)}, \quad (43)$$

where l is still the semi-latus rectum. It is now possible to calculate the power emitted per unit angle ϕ . To that end, we must first compute the energy and angular momentum (per unit mass) of a body in a gravitational potential $\Phi(r)$ [6]:

$$E = \frac{1}{2}v^2 + \Phi(r) = \frac{1}{2} \left[\left(\frac{dr}{dt} \right)^2 + r^2 \left(\frac{d\phi}{dt} \right)^2 \right] + \Phi(r), \quad (44)$$

$$L = \vec{r} \times \vec{v} = r^2 \frac{d\phi}{dt}. \quad (45)$$

Putting these equations together and substituting $u = 1/r$, we obtain

$$\frac{2E}{L^2} = \left(\frac{du}{d\phi} \right)^2 + u^2 + \frac{2\Phi}{L^2}. \quad (46)$$

Since the specific energy E and the angular momentum L are conserved quantities, the derivative of the last expression should equal zero. More precisely, this results in the differential equation

$$\frac{d^2u}{d\phi^2} + u = \frac{Gm_2}{L^2}, \quad (47)$$

which has the following solution:

$$u(\varphi) = A \cos(\varphi - \varphi_0) + \frac{Gm_2}{L^2} \iff \frac{dr}{dt} = BL \sin(\varphi - \varphi_0). \quad (48)$$

In this equation, A is a constant depending on the initial conditions and φ_0 , as shown in figure 8, is the angle corresponding to the closest approach of m_1 to m_2 , at $r_{min} = a(1 - e)$. There exists a relation between the eccentricity and φ , which is explicitly given as [8]

$$e = \frac{-1}{\cos \varphi_0}. \quad (49)$$

Just like in the circular case (section 2.3) and in the elliptical case (section 3), we will transform the problem to a reduced-mass problem. The orbit of a reduced-mass particle reads [21]:

$$r = \frac{b \sin \varphi_0}{\cos(\varphi - \varphi_0) - \cos \varphi_0}. \quad (50)$$

Like before, we need to calculate the components of the quadrupole moment, using the definition in equation (11) or an equivalent one. The x_i in that definition correspond to the usual Cartesian coordination, but it is more convenient to rewrite them to their spherical equivalents in this case. Taking note that we are in the xy-plane, which means $z = 0$ and $\theta = \frac{\pi}{2}$, the relations are

$$x = r \cos \varphi \sin \theta = r \cos \varphi, \quad (51a)$$

$$y = r \sin \varphi \sin \theta = r \sin \varphi, \quad (51b)$$

$$z = 0. \quad (51c)$$

We can now calculate the components of the quadrupole moment. Interestingly, they are identical in form to the ones found in the elliptical case (see eqs. (27)):

$$Q_{xx} = \mu r^2 \cos^2 \varphi, \quad (52a)$$

$$Q_{yy} = \mu r^2 \sin^2 \varphi, \quad (52b)$$

$$Q_{xy} = Q_{yx} = \mu r^2 \sin \varphi \cos \varphi. \quad (52c)$$

Taking the third time-derivative, so that we may apply the quadrupole formula (19), we find that the power emitted per unit angle of the hyperbolic encounter is given by (see [6], [8]):

$$P(\varphi) = -\frac{32GL^6\mu^2}{45c^5b^8} f(\varphi, \varphi_0). \quad (53)$$

where the final factor is given by

$$f(\varphi, \varphi_0) = \frac{\sin(\varphi_0 - \frac{\varphi}{2})^4 \sin(\frac{\varphi}{2})^4}{\tan(\varphi_0)^2 \sin(\varphi_0)^6} \cdot \left[150 + 72 \cos(2\varphi_0) + 66 \cos(2(\varphi_0 - \varphi)) - \right. \\ \left. - 144(\cos(2\varphi_0 - \varphi) - \cos(\varphi)) \right]. \quad (54)$$

In figure 9 below, we plot the power radiated as a function of the angle, normalised by the maximum power which occurs at closest approach, at an angle of $\varphi_0 = 0.6\pi$.

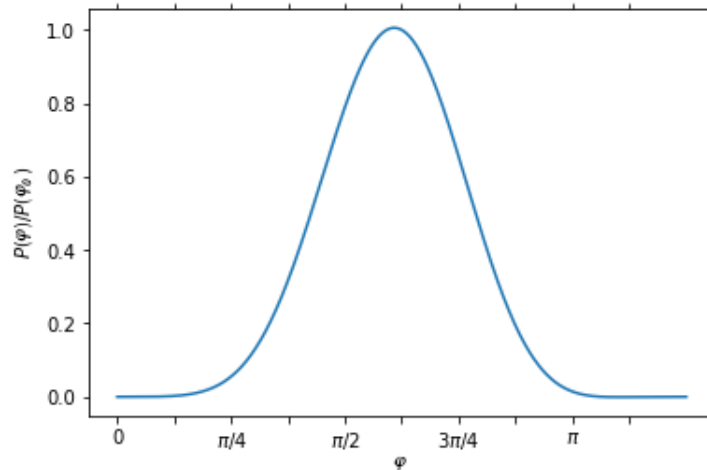


Figure 9: Power as a function of the angle φ during a hyperbolic approach, with an angle of closest approach of $\varphi_0 = 0.6\pi$. (from [8])

One might wonder how much energy is radiated in total during a hyperbolic approach, and this may be calculated by integrating the power $P = \frac{dE}{dt}$ over all of time, i.e. $t \in (-\infty, \infty)$. Expression (53) is a function of angle, so to integrate over time, we must make a change of variables. The result we find, after implementing the definition of the angular momentum $L = \mu bv_0$, is [8]:

$$\Delta E = \frac{32G\mu^2 v_0^6}{bc^5} F(\varphi_0), \quad (55)$$

where the final factor is now solely dependent on the angle of closest approach φ_0 , and is given by

$$F(\varphi_0) = \frac{2628\varphi_0 + 2328\varphi_0 \cos(2\varphi_0) + 144\varphi_0 \cos(4\varphi_0) - 1948 \sin(2\varphi_0) - 301 \sin 4\varphi_0}{720 \tan^2(\varphi_0) \sin^4(\varphi_0)}. \quad (56)$$

Taking the same value for φ_0 as before, we can try and obtain a few example values for how much energy might be radiated. As is clear from expression (55), it is heavily dependent on the initial velocity v_0 , which would be the velocity of mass m_1 at infinity. Seeing as the wave packets or bursts resulting from these encounter would be rather short in duration, it is hard to detect them and to obtain realistic estimates for the parameters. So, choosing $m_1 = m_2 = 30M_\odot$, an initial velocity of $v_0 = 200$ km/s and an impact parameter of $b = 0.001$ AU, we obtain a value for the total energy radiated of $\Delta E \approx 3.5 \cdot 10^{26}$ J, which is around one second worth of solar luminosity. The peak power can be easily found by differentiating the power equation (53) with respect to the angle φ and setting equal to zero. With the parameters listed, the peak power is $P_{max} \approx 2.410^{23}$ W, or about 1500 times less than L_\odot .

However, if we imagine a scenario with identical masses, but with an initial velocity $v_0 = 0.01c$, an impact parameter of $b = 0.01$ AU and an orbital eccentricity of $e = 1.1$,

we find a peak power of $P_{max} \approx 2 \cdot 10^{35}$ W, or about $10^9 L_\odot$. This figure seems a lot more detectable even at cosmic distances. We can calculate the maximum gravitational wave strain for such a scenario through equation (18), where we perform the summation over $i, j = 1, 2$, i.e.

$$h_{total}^{max} = \frac{2G}{c^4 d_L} \left\langle \frac{d^2 Q_{ij}}{dt^2} \frac{d^2 Q^{ij}}{dt^2} \right\rangle^{1/2}. \quad (57)$$

Evaluating for the particular case described above, at a luminosity distance of $d_L = 1$ Gpc, we find a maximum gravitational wave strain of $h_{total}^{max} \approx 2 \cdot 10^{-23}$, which is just inside the range of sensitivity of Advanced LIGO [17]. More on the possibility of detection of these encounter in the discussion in section 4.

4 Discussion and conclusions

In this thesis, we examined and confirmed the theoretical framework of gravitational wave emission of binary black holes, by starting out at the simple case of circular orbits, and then examining to the more realistic case of elliptical orbits, both bound and unbound. It was found that the power of gravitational radiation in the bound elliptical case is equal to the circular case, times an enhancement factor solely dependent on the eccentricity of the orbit, which is a result that is corroborated by various researchers before us (see e.g. [19]). Changes in the orbital parameters of such a system were examined as well, and it was found that both the semi-major axis a and the eccentricity e strictly decrease with time, which matches intuition, because these systems must eventually spiral into one another and merge. These findings were also previously confirmed by other researchers (see e.g. [16]).

At the end of section 3.1, a way to determine the time scales on which binary systems of black holes, of equal masses $m_1 = m_2 = 30M_\odot$ was given for an initial orbital frequency of 1 Hz. Though no statement was made on how such a system might emerge, it was found that a system that still has an orbital eccentricity of $e = 0.1$ by the time it reaches an orbital frequency of 1 Hz, will take about 10^5 seconds, or roughly 28 hours to achieve an increase of a factor of roughly 10^2 which was found to be the maximum orbital frequency reached by GW150914, which consisted of black holes of similar mass [7].

Furthermore, an analysis of the gravitational wave emission for hyperbolic encounters was provided, and an expression for the GW power of such scenarios was given, as was also found by researchers before. It was found that the peak power of the gravitational radiation coincides with the closest approach of the two bodies, which satisfies one's intuition, as one would expect the peak acceleration of the approaching body to be at the periastron. A few numerical examples were calculated, and a case which would already be detectable (superficially speaking) was found in section 3.2.

The issue of detecting such events goes beyond the gravitational wave strain falling within the range of sensitivity of observational arrays. In the case of the hyperbolic encounter, one of the other difficulties lies in the duration of the event. As found by García-Bellido & Nesseris [12], it takes only on the order of tens of milliseconds for the power of these events to go from their maximum to half of it. This makes observing them rather difficult, as they could be mistaken for noise, and there aren't more opportunities to observe the system in a later stage, as one might be able to do in a bound system. However, assuming one happens to detect such an encounter, there is research that specifies the spectrum of the gravitational waves emitted (see e.g. [8]), which might help to identify these scenarios.

References

- [1] Supplement to chapter 23 : The derivation of the quadrupole formula. URL <http://web.physics.ucsb.edu/~gravitybook/websups/Ch23.pdf>.
- [2] What are gravitational waves? URL <http://public.virgo-gw.eu/what-are-gravitational-waves/>.
- [3] B. P. Abbott, R. Abbott, T. D. Abbott, M. R. Abernathy, F. Acernese, K. Ackley, C. Adams, Adams, and et al. Observation of gravitational waves from a binary black hole merger. *Phys. Rev. Lett.*, 116:061102, Feb 2016. doi: 10.1103/PhysRevLett.116.061102. URL <https://link.aps.org/doi/10.1103/PhysRevLett.116.061102>.
- [4] B. P. Abbott, R. Abbott, T. D. Abbott, M. R. Abernathy, F. Acernese, K. Ackley, C. Adams, T. Adams, P. Addesso, and et al. The basic physics of the binary black hole merger gw150914. *Annalen der Physik*, 529(1-2):1600209, Oct 2016. ISSN 0003-3804. doi: 10.1002/andp.201600209. URL <http://dx.doi.org/10.1002/andp.201600209>.
- [5] L. Baiotti and L. Rezzolla. Binary neutron star mergers: a review of einstein’s richest laboratory. *Reports on Progress in Physics*, 80(9):096901, Jul 2017. ISSN 1361-6633. doi: 10.1088/1361-6633/aa67bb. URL <http://dx.doi.org/10.1088/1361-6633/aa67bb>.
- [6] S. Capozziello, M. De Laurentis, F. De Paolis, G. Ingrosso, and A. Nucita. Gravitational waves from hyperbolic encounters. *Modern Physics Letters A*, 23(02):99–107, Jan 2008. ISSN 1793-6632. doi: 10.1142/s0217732308026236. URL <http://dx.doi.org/10.1142/S0217732308026236>.
- [7] G. Carullo, G. Riemenschneider, K. W. Tsang, A. Nagar, and W. Del Pozzo. Gw150914 peak frequency: a novel consistency test of strong-field general relativity. *Classical and Quantum Gravity*, 36(10):105009, Apr 2019. ISSN 1361-6382. doi: 10.1088/1361-6382/ab185e. URL <http://dx.doi.org/10.1088/1361-6382/ab185e>.
- [8] L. De Vittori, P. Jetzer, and A. Klein. Gravitational wave energy spectrum of hyperbolic encounters. *Physical Review D*, 86(4), Aug 2012. ISSN 1550-2368. doi: 10.1103/physrevd.86.044017. URL <http://dx.doi.org/10.1103/PhysRevD.86.044017>.
- [9] A. Einstein. Näherungsweise integration der feldgleichungen der gravitation. 1916. Bibcode 1916SPAW.....688E.
- [10] A. Einstein. Über gravitationswellen. 1918. Bibcode 1918SPAW.....154E.
- [11] M. Enoki and M. Nagashima. The effect of orbital eccentricity on gravitational wave background radiation from supermassive black hole binaries. *Progress of Theoretical Physics*, 117(2):241–256, Feb 2007. ISSN 1347-4081. doi: 10.1143/ptp.117.241. URL <http://dx.doi.org/10.1143/PTP.117.241>.
- [12] J. García-Bellido and S. Nesseris. Gravitational wave energy emission and detection rates of Primordial Black Hole hyperbolic encounters. *Phys. Dark Univ.*, 21:61–69, 2018. doi: 10.1016/j.dark.2018.06.001.

- [13] J. B. Hartle. *Gravity: An Introduction to Einstein's General Relativity*. Pearson, 1 edition, 2014.
- [14] M. E. Lower, E. Thrane, P. D. Lasky, and R. Smith. Measuring eccentricity in binary black hole inspirals with gravitational waves. *Physical Review D*, 98(8), Oct 2018. ISSN 2470-0029. doi: 10.1103/physrevd.98.083028. URL <http://dx.doi.org/10.1103/PhysRevD.98.083028>.
- [15] M. Maggiore. *Gravitational Waves. Volume 1: Theory and Experiments*. Oxford University Press, 2007.
- [16] K. Martel and E. Poisson. Gravitational waves from eccentric compact binaries: Reduction in signal-to-noise ratio due to nonoptimal signal processing. *Physical Review D*, 60(12), Nov 1999. ISSN 1089-4918. doi: 10.1103/physrevd.60.124008. URL <http://dx.doi.org/10.1103/PhysRevD.60.124008>.
- [17] D. Martynov, E. Hall, B. Abbott, R. Abbott, T. Abbott, C. Adams, R. Adhikari, R. Anderson, S. Anderson, K. Arai, and et al. Sensitivity of the advanced ligo detectors at the beginning of gravitational wave astronomy. *Physical Review D*, 93(11), Jun 2016. ISSN 2470-0029. doi: 10.1103/physrevd.93.112004. URL <http://dx.doi.org/10.1103/PhysRevD.93.112004>.
- [18] P. Peters and J. Mathews. Gravitational radiation from point masses in keplerian orbit. *The Physical Review*, 131(1):435–440, Jul 1963.
- [19] P. C. Peters. *Gravitational Radiation and The Motion of Two Point Masses*. PhD thesis, California Institute of Technology, 2 1964.
- [20] A. Shields, R. Barnes, E. Agol, B. Charnay, C. Bitz, and V. Meadows. The effect of orbital configuration on the possible climates and habitability of kepler-62f. *Astrobiology*, 16, 03 2016. doi: 10.1089/ast.2015.1353.
- [21] W. M. Smart. *Textbook on Spherical Astronomy*. Cambridge University Press, 6 edition, 1977. doi: 10.1017/CBO9781139167574.
- [22] J. Taylor, L. Fowler, and P. McCulloch. Measurements of general relativistic effects in the binary pulsar psr1913 + 16. *Nature*, (277):437–440, 1979.
- [23] M. Turner. Gravitational radiation from point-masses in unbound orbits: Newtonian results*. *The Astrophysical Journal*, 216:610–619, Sep 1977.

A Appendix

As stated before, there would be some derivations for used quantities listed. We first give a derivation of equation (18) and then a derivation for the quadrupole formula, equation (19).

A.1 Gravitational wave strain

The derivation for this quantity can be largely found in Hartle's Gravity [13], but is shown a bit more extensively here, for clarity's sake. Here, $h^{\alpha\beta}$ is the gravitational wave strain, and $T^{\alpha\beta}$ is the stress-energy tensor. The general solution of the linearised Einstein equations (from Hartle p.498 [13]) is:

$$h^{\alpha\beta}(t, \vec{x}) = 4 \int d^3x' \frac{[T^{\alpha\beta}(t', \vec{x}')]_{ret}}{|\vec{x} - \vec{x}'|}, \quad (58)$$

where $[\cdot]_{ret}$ is taken to mean that the argument should be evaluated at the retarded time, i.e.

$$t' = t_{ret} = t - |\vec{x} - \vec{x}'|. \quad (59)$$

Now, let's assume we're a large distance r away from the source of the gravitational waves, and that the source is a rather weak one, meaning that the orbital velocities of its constituents are non-relativistic:

$$r \gg R_{source},$$

$$\lambda = \frac{2\pi}{\omega_{source}} \gg R_{source}.$$

where R_{source} and ω_{source} are the characteristic size and the characteristic orbital frequency of the source respectively. This allows us to set $|\vec{x} - \vec{x}'| = r$, whereby equation (58) reduces to

$$h^{\alpha\beta}(t, \vec{x}) \xrightarrow{r \rightarrow \infty} \frac{4}{r} \int d^3x' T^{\alpha\beta}(t - r, \vec{x}'). \quad (60)$$

Seeing as we're indeed far from the source, we can assume our local space-time to be (mostly) flat. That means we have conservation of energy/momentum of matter,

$$\frac{\partial T^{\alpha\beta}}{\partial x^\beta} = 0. \quad (61)$$

One component of this equation, in linear order of the spatial components of $h^{\alpha\beta}$, i.e., h^{ij} , is

$$\frac{\partial T^{tt}}{\partial t} + \frac{\partial T^{kt}}{\partial x^k} = 0. \quad (62)$$

Using the symmetry of the stress-energy tensor $T^{tk} = T^{kt}$, the conservation law in (62) once again and differentiating the equation above with respect to time, we find:

$$\begin{aligned} \frac{\partial^2 T^{tt}}{\partial t^2} &= -\frac{\partial}{\partial t} \left(\frac{\partial T^{tk}}{\partial x^k} \right) = -\frac{\partial}{\partial x^k} \left(\frac{\partial T^{tk}}{\partial t} \right) \\ &= \frac{\partial^2 T^{kl}}{\partial x^k \partial x^l}. \end{aligned} \quad (63)$$

Multiply both sides of the equation above by $x^i x^j$ and integrate over space (d^3x). The integration of the right-hand side ought to be carried out parts, and the surface terms shall be found to vanish:

$$\int d^3x \frac{\partial^2 T^{tt}(x)}{\partial t^2} x^i x^j = \int d^3x \frac{\partial^2 T^{kl}}{\partial x^k \partial x^l} x^i x^j, \quad (64)$$

$$\implies \frac{1}{2} \frac{d^2}{dt^2} \int d^3x T^{tt}(x) x^i x^j = \int d^3x T^{ij}(x). \quad (65)$$

Long wavelengths mean low velocities, as mentioned before, which means the stress-energy tensor has the form $T^{\alpha\beta}(x) = \mu(x) u^\alpha u^\beta$, where u^α are non-relativistic four-velocities. The energy density $T^{tt}(x)$ will then be dominated by the rest-mass density $\mu(x)$ and the integral above in (65) defines the second mass moment, i.e. the quadrupole moment tensor Q^{ij} :

$$Q^{ij} = \int d^3x \mu(t, \vec{x}) x^i x^j, \quad (66)$$

Which is not quite the same as what's written down in equation (11), which is the reduced form of the quadrupole moment tensor, and has been made traceless, but the one tensor can be constructed from the other. What we're left with now, by plugging the expression for T^{ij} back into equation (60), is:

$$h^{ij} \xrightarrow{r \rightarrow \infty} \frac{4}{r} \frac{1}{2} \frac{d^2}{dt^2} \int d^3x \mu(t, \vec{x}) x^i x^j = \frac{2}{r} \ddot{Q}^{ij}, \quad (67)$$

which, if we understand these equations to be written in units of $G = c = 1$, and take $r = d_L$ as before, gives us exactly equation (18).

A.2 Quadrupole formula

We can now continue the derivation of the quadrupole formula (19), in which we can use our previous result. This derivation large follows the approach from both Hartle's *Gravity* [13] and the supplement to it found in [1], but is a little more fleshed out in places.

To derive the quadrupole formula, we'll first need to find an energy flux, which Hartle states to be possible directly from the stress-energy tensor of a linearised plane GW. We may find that tensor by examining the Einstein equation, and noting that, for the metric $g_{\mu\nu}(x)$ in absence of other sources, it reduces down to

$$R_{\mu\nu}(g) = 0, \quad (68)$$

where $R_{\mu\nu}(g)$ means all components of $R_{\mu\nu}$ depend on all 10 components of $g_{ij}(x)$. Linearisation allows us to write the metric as

$$g_{\mu\nu}(x) = \gamma_{\mu\nu}(x) + h_{\mu\nu}(x), \quad (69)$$

where $\gamma_{\mu\nu}$ is a smooth background (B) metric, and $h_{\mu\nu}$ is a small ripple propagating through space-time. Let's expand equation (69) in powers of the amplitude of the wave $h_{\mu\nu}$, and we find

$$R_{\mu\nu} = R_{\mu\nu}^{(B)}(\gamma) + R_{\mu\nu}^{(1)}(\gamma, h) + R_{\mu\nu}^{(2)}(\gamma, h) + \dots = 0. \quad (70)$$

Here, the first term is the curvature of the smooth background, the second is linear in $h_{\mu\nu}$, and the second term is quadratic in $h_{\mu\nu}$. We can neglect higher order terms. If the background metric is curved solely by the energy in the wave propagating through space-time, it can't be a linear effect, because the energy in the wave is quadratic. Therefore, the linear term must vanish by itself:

$$R_{\mu\nu}^{(1)}(\gamma, h) = 0. \quad (71)$$

The terms left can only be equal in an average sense, due to the difference in exponent and what that entails for the frequency of the waves travelling through space-time. Let's denote an average over a space-time volume with sides larger than a wavelength as $\langle \cdot \rangle$, and write:

$$R_{\mu\nu}^{(B)}(\gamma) = -\langle R_{\mu\nu}^{(2)}(\gamma, h) \rangle. \quad (72)$$

This shows how quadratic terms in the amplitude of the GW generate space-time curvature. We can make this identification explicit by writing (72) in the form of an Einstein equation. The ordinary Einstein equation reads:

$$R_{\alpha\beta} - \frac{1}{2}g_{\alpha\beta}R = 8\pi GT_{\alpha\beta}. \quad (73)$$

Applying this same form to (72) yields:

$$R_{\mu\nu}^{(B)}(\gamma) = 8\pi \left(T_{\mu\nu}^{(GW)} - \frac{1}{2}\gamma_{\mu\nu}T^{(GW)} \right), \quad (74)$$

where $T^{(GW)} = T_{\rho}^{\rho}$ is a scalar, so that the effective gravitational wave stress-energy tensor is

$$T_{\mu\nu}^{(GW)} = -\frac{1}{8\pi} \left[\langle R_{\mu\nu}^{(2)} \rangle - \frac{1}{2}\gamma_{\mu\nu}\langle R^2 \rangle \right]. \quad (75)$$

Let's now try and calculate this for plane linearised GW, i.e. with

$$h_{\mu\nu} = \begin{pmatrix} 0 & 0 & 0 & 0 \\ 0 & 1 & 0 & 0 \\ 0 & 0 & 1 & 0 \\ 0 & 0 & 0 & 0 \end{pmatrix} f(t - z), \quad (76)$$

where $f(t - z)$ is some function of $(t - z)$, which will realistically in this case be $f(t - z) = a \sin(\omega(t - z))$. The energy flux is the component $T_{(GW)}^{tz}$, which we can calculate with $\gamma_{\mu\nu} = \eta_{\mu\nu}$, the ordinary flat metric. To calculate the Ricci curvature, we need to calculate Christoffel symbols given in terms of the metric. This is in principle a straightforward process, but also a rather tedious one, so let's make our lives a little easier by seeing which elements we can get away with not calculating. The wave $h_{\mu\nu}$ has no components except in the transverse x- and y-directions. That is enough to show that $\Gamma_{tz}^{\alpha} = \Gamma_{tt}^{\alpha} = \Gamma_{zz}^{\alpha} = 0$. Together with $g^{\alpha\gamma}g_{\alpha\beta} = \delta_{\gamma}^{\alpha}$, we can establish up to first order in $h_{\mu\nu}$:

$$g_{(1)}^{\mu\nu} = -h^{\mu\nu}, \quad (77)$$

where the indices are raised through the use of the metric tensor $\eta^{\mu\nu}$:

$$h^{\mu\nu} = \eta^{\mu\gamma}\eta^{\nu\rho}h_{\gamma\rho}. \quad (78)$$

Putting all this together, one finds an expression for a component of the Ricci curvature tensor:

$$R_{tz} = \frac{1}{4} \frac{\partial h_{ij}}{\partial t} \frac{\partial h_{ij}}{\partial z} = \frac{1}{2} h^{ij} \frac{\partial^2 h_{ij}}{\partial t \partial z}. \quad (79)$$

Now, putting in a wave of the form of equation (76), averaging over a period (granting a numerical factor), and raising indices using $\eta^{\mu\nu}$ like before, we find:

$$\begin{aligned} T_{(GW)}^{tz} &= -\frac{1}{8\pi} \left[\langle R_{tz}^{(GW)} \rangle - \frac{1}{2} \gamma_{tz} \langle R^2 \rangle \right] \\ &= \frac{\omega^2}{32\pi} \langle h_{ij} h^{ij} \rangle \\ &= \frac{\omega^2 a^2}{32\pi}. \end{aligned} \quad (80)$$

Thereby we have found an energy flux, which we can use to find an expression for the flux in the direction of an arbitrary unit vector n^i , and then integrate over all directions to find the total radiated power. We will continue with the choice of metric as before, but we will choose to switch to the Transverse Traceless (TT) gauge. There, $h_{\mu\nu}$ is expressed as

$$h_{\mu\nu}^{TT}(x) = \begin{pmatrix} 0 & 0 & 0 & 0 \\ 0 & a & b & 0 \\ 0 & b & -a & 0 \\ 0 & 0 & 0 & 0 \end{pmatrix} e^{i\omega(z-t)}, \quad (81)$$

so that still $a^2 = \langle h_{\mu\nu}^{TT} h_{TT}^{\mu\nu} \rangle$, as the sums over μ and ν produce $2a^2$ and the time averaging $\langle \cdot \rangle$ gives $\frac{1}{2}$. Then we may find that the energy flux in direction of an arbitrary unit vector n^i is

$$\Pi_{GW}^i = \frac{\omega^2}{32\pi} n^i \langle h_{\mu\nu}^{TT} h_{TT}^{\mu\nu} \rangle. \quad (82)$$

It is common to write the spatial components $h_{\mu\nu}^{TT}$ differently (note that it remains invariant under transversion and it remains traceless):

$$h_{ij}^{TT} = \begin{pmatrix} \frac{1}{2}(h_{xx} - h_{yy}) & h_{xy} & 0 \\ h_{xy} & \frac{1}{2}(h_{yy} - h_{xx}) & 0 \\ 0 & 0 & 0 \end{pmatrix}. \quad (83)$$

With (82) and (83), we can evaluate this flux in z-direction in terms of the mass quadrupole moment, noting that $\ddot{Q}_{ij} = -\omega^2 Q_{ij}$ for a periodic source. Then

$$\Pi_{GW}^z = \frac{\omega^6}{32\pi} \langle 2(Q_{xx} - Q_{yy})^2 + 8I_{xy}^2 \rangle. \quad (84)$$

Here it's convenient to switch to the reduced mass quadrupole moment, as it is traceless. It is defined as

$$\tilde{Q}_{ij} = Q_{ij} - \frac{1}{3} \delta_{ij} Q_k^k. \quad (85)$$

We can put this back into equation (84) and see that

$$\begin{aligned}\Pi_{GW}^z &= \frac{\omega^6}{32\pi r^2} \langle (\tilde{Q}_{xx} - \tilde{Q}_{yy})^2 + 8\tilde{Q}_{xy}^2 \rangle \\ &= \frac{\omega^6}{16\pi r^2} \langle 2\tilde{Q}_{ij}\tilde{Q}^{ij} - 4\tilde{Q}_{zi}\tilde{Q}_z^i - \tilde{Q}_{zz}^2 \rangle.\end{aligned}\tag{86}$$

This can be checked by filling in $\tilde{Q}_k^k = \tilde{Q}_{xx} + \tilde{Q}_{yy} + \tilde{Q}_{zz}$, which we won't do here for the sake of brevity. Now we can find the energy flux in any direction:

$$\Pi_{GW}^i n^i = \frac{\omega^6}{16\pi r^2} \langle 2\tilde{Q}_{ij}\tilde{Q}^{ij} - 4(\tilde{Q}_{ik}n^k)(\tilde{Q}_l^i n^l) - (\tilde{Q}_{ij}n^i n^j) \rangle.\tag{87}$$

The next step is to do the angular integration, i.e.

$$\frac{dE}{dt} = \int r^2 \Pi_{GW}^i n^i d\Omega_{\vec{n}}.\tag{88}$$

Beyond the usual $\int d\Omega_{\vec{n}} = 4\pi$, there are two more types of angular integration:

$$\mathcal{A}^{ij} = \int d\Omega_{\vec{n}} n^i n^j,\tag{89a}$$

$$\mathcal{B}^{ijkl} = \int d\Omega_{\vec{n}} n^i n^j n^k n^l.\tag{89b}$$

We can rewrite (88) in terms of these two integrations:

$$\frac{dE}{dt} = \frac{\omega^6}{16\pi} \langle 8\pi\tilde{Q}_{ij}\tilde{Q}^{ij} - 4\tilde{Q}_l^i \mathcal{A}^{kl} - \tilde{Q}_{ij}\tilde{Q}_{kl} \mathcal{B}^{ijkl} \rangle.\tag{90}$$

We can once again save ourselves a bit of suffering by thinking rather than blindly computing. These integrals cannot depend on \vec{n} , as that's being integrated over. They can only be constructed out of Kronecker delta's in such a way as to reflect the symmetries of the integrals themselves, i.e.:

$$\mathcal{A}^{ij} = A\delta^{ij},\tag{91a}$$

$$\mathcal{B}^{ijkl} = B(\delta^{ij}\delta^{kl} + \delta^{il}\delta^{jk} + \delta^{ik}\delta^{jl}),\tag{91b}$$

where A and B are now numerical coefficients which can be determined through two integrals:

$$\mathcal{A}_i^i = \int d\Omega_{vecn} = 4\pi, \quad (92)$$

but also note that $\mathcal{A}_i^i = 3A$, so that we find $A = \frac{4\pi}{3}$. In a similar fashion, we find that $B = \frac{4\pi}{15}$, so that in total have that

$$\mathcal{A}^{ij} = \frac{4\pi}{3}\delta^{ij}, \quad (93a)$$

$$\mathcal{B}^{ijkl} = \frac{4\pi}{15}(\delta^{ij}\delta^{kl} + \delta^{il}\delta^{jk} + \delta^{ik}\delta^{jl}). \quad (93b)$$

This now allows us to evaluate equation (90) with relative ease, so that we can conclude that the radiated power depends only on $\tilde{Q}_{ij}\tilde{Q}^{ij}$:

$$\frac{dE}{dt} = \frac{\omega^6}{5}\langle\tilde{Q}_{ij}\tilde{Q}^{ij}\rangle. \quad (94)$$

This doesn't immediately look similar to equation (19), but note that deriving \tilde{Q}_{ij} with respect to time moves a factor ω forward. Doing that, and keeping in mind that we are in units of $c = G = 1$, we have successfully derived the quadrupole formula (19).